Chemical Engineering Journal 162 (2010) 730–737

Contents lists available at ScienceDirect

Chemical Engineering Journal

journal homepage: www.elsevier.com/locate/cej

Shape optimization of a micromixer with staggered-herringbone grooves patterned on opposite walls

Shakhawat Hossain, Afzal Husain, Kwang-Yong Kim*

Department of Mechanical Engineering, Inha University, 253 Yonghyun-Dong Nam-Gu, Incheon 402-751, Republic of Korea

ARTICLE INFO

Article history:
Received 24 November 2009
Received in revised form 21 May 2010
Accepted 28 May 2010

Keywords:
Micromixer
Herringbone grooves
Optimization
Navier–Stokes equations
Mixing index
Response surface method

ABSTRACT

The shape optimization of a micromixer with staggered-herringbone grooves at both the top and bottom walls has been performed through three-dimensional Navier–Stokes analysis. The mixing of two working fluids, viz., water and ethanol, is considered at Re = 1. The mixing index at the exit of the micromixer is selected as the objective function and four design variables, viz., the number of grooves per half cycle, angle of grooves, ratio of the groove depth to channel height, and ratio of the groove width to pitch are chosen out of the various geometric parameters that affect the performance of a micromixer with regard to shape optimization. The variance of the mass-fraction at various nodes on a plane is used to quantify the mixing performance in the micromixer. The design space is explored through some preliminary calculations and a Latin hypercube sampling method is used as the design of experiments to select design points in the design space. The objective function values are obtained at these design points by Navier–Stokes analysis, and a surrogate model, namely, the response surface approximation method, is used to construct a response surface for the objective function. Sequential quadratic programming is used to find out an optimal solution on the constructed response space. The optimization results show that the mixing is highly sensitive to the shape of the groove as well as the number of grooves per cycle, which can be used to control mixing in microfluidics. Through the optimization, the mixing index at the exit of the micromixer is enhanced by about 9% in comparison with the reference design.

1. Introduction

Rapid mixing is a fundamental requirement for any microfluidic system that deals with chemical synthesis, drug delivery, high-throughput screening, and biochemistry. In microsystems, due to their small sizes, fluid mixing becomes very difficult, and conventional methods for stirring fluids are not applicable for carrying out the required mixing. Mixing in microchannels is predominantly governed by molecular diffusion, which in itself is a very slow process; it can be improved by increasing the area of the contact interface between the fluids and decreasing the diffusion path. Microfluidic devices are used to perform many functions such as separation, mixing, reaction, and analysis on a single chip; therefore, mixing in microchannels plays an important role in realizing BioMEMS and micro total analysis systems [1,2].

Recently, a variety of active and passive micromixers have been developed to enhance fluid mixing in microchannels. Active micromixers depend on external effects to force fluids to mix together inside the microchannels [3,4]. To enhance the mixing performance in an active micromixer, the stirring effect can be achieved by using additional structures or external sources, including ultrasonic vibration, dielectrophoresis, electrohydrodynamics, electroosmosis, and magnetic-force techniques. Passive micromixers do not require any external energy other than the fluid drive: the mixing process is achieved by modifying the microchannel geometry with different shapes or microstructures. Due to various complications that are involved in active micromixers, passive micromixers are used in most microfluidic applications.

The patterning of one or more surfaces of the micromixer by specially designed microstructures is one of the best procedures for enhancing the mixing performance of a passive micromixer. Stroock et al. [5] developed a novel type of T-shaped micromixer, which uses patterned grooves at the bottom of the channel; they reported that the groove shape could be very effective in mixing fluids. This micromixer creates a transverse flow pattern that stretches and folds the fluids, which increases the mixing performance. Wang et al. [6] investigated the mixing performance by using the computational fluid dynamics (CFD) method for a patterned-groove micromixer and reported that deeper grooves improved the mixing efficiency and reduced the channel length for complete mixing. The mixing of fluids in a herringbone-groove micromixer depends upon the geometric parameter of the herringbone grooves that represents their patterning, shape, and size.

* Corresponding author. Tel.: +82 32 872 3096; fax: +82 32 868 1716.
E-mail address: kykim@inha.ac.kr (K.-Y. Kim).

1385-8947/$ – see front matter © 2010 Elsevier B.V. All rights reserved.
doi:10.1016/j.cej.2010.05.056

Nomenclature

d	depth of grooves
h	channel height
Li	inlet channel length
Lm	main channel length
Lo	channel exit length
M	mixing index
N	number of grooves per half cycle
N_o	number of sampling points
Pi	groove pitch
q	wave vector of ridges
Re	Reynolds number
R^2_{adj}	adjusted R square
W	channel width
Wd	width of grooves
x, y, z	streamwise, spanwise, and cross-streamwise coordinates, respectively

Greek letters

θ	angle of the grooves
μ	absolute viscosity of fluid ($Kg\,m^{-1}\,s^{-1}$)
ρ	fluid density ($Kg\,m^{-3}$)
σ	variance

Subscripts

i	sampling point
max	maximum value
min	minimum value
N–S	Navier–Stokes
opt	optimum value
x	axial distance

A numerical investigation has been performed by Liu et al. [7] to observe the influence of different fluid properties and a large concentration gradient on the mixing behavior of two miscible fluids for a three-dimensional serpentine mixer and a micromixer with staggered-herringbone grooves (SHGs) at Re = 1 and 10. Kang and Kwon [8] performed numerical simulation with three different patterned-groove micromixers: a slanted-groove micromixer, a staggered-herringbone micromixer, and a barrier-embedded micromixer. A particle tracking method was applied to visualize and quantify the mixing of the two different fluids.

The effects of geometric parameters on the mixing performance of an SHG mixer with patterned grooves were numerically investigated by Yang et al. [9]. Analyses of the mixing phenomena, pressure loss, and flow rate through grooves were also performed. To improve the mixing quality in a staggered-herringbone micromixer, Aubin et al. [10] numerically investigated the effects of the different geometrical parameters of an SHG micromixer and reported that the mixing performance depends on the geometric parameters of the grooves. To examine the relationship between the dimensions of a patterned-groove micromixer and fluid rotation in the micromixer, a numerical study has been performed by Tang et al. [11]. A parametric study for a micromixer patterned with three grooves was performed by Hassell and Zimmerman [12] for different groove depths and Reynolds numbers.

Howell et al. [13] studied a mixer design based on the placement of grooves at both the top and bottom walls of the channel. A patterned-groove micromixer with a combination of chevron grooves and angled grooves was studied through CFD simulation. Yang et al. [14] studied a novel mixing device with connected grooves named a connected-groove micromixer (CGM), and reported that it creates a helical flow with a short pitch and generates an intense transverse field that enhances the mixing.

An optimization study has been performed by Johnson and Locascio [15] on a slanted-groove micromixer under electroosmotic flow. They reported that the mixing performance is enhanced by increasing the depth and decreasing the inclination (angle formed between the groove and the channel) of the grooves. Ansari and Kim [16] used a numerical optimization technique to enhance the mixing performance by optimizing the shape of an SHG mixer with grooves on the bottom wall. The authors applied the Radial Basis Neural Network method to optimize the groove shape with three design variables, viz., the ratio of the groove depth to channel height, angle of grooves, and ratio of the groove width to pitch. Ansari and Kim [17] has applied the response surface approximation (RSA) method as a numerical optimization tool to obtain the optimal groove shape by using two design variables, viz., the ratio of the groove depth to channel height and the angle of grooves. Their sensitivity analysis revealed that mixing was more sensitive to the ratio of the groove depth to channel height than the angle of grooves.

The optimization of helical flow within a slanted-groove mixer has been performed by Lynn and Dandy [18]. They reported that the mixing is strongly affected by the aspect ratio, the groove depth ratio, and the ridge length. An optimization analysis of a staggered-herringbone micromixer was executed by Song et al. [19] based on the slip-driven method. The slip-driven method was used to simplify the 3D flow in the staggered-herringbone micromixer into a 2D cavity flow with an axial Poiseuille flow. The effects of geometric parameters on the mixing performance of an SHG mixer based on the generation of chaotic advection have been evaluated numerically by Quiroz et al. [20]. The authors applied a multi-objective optimization technique to enhance the mixing performance and optimize the geometric parameters. Two objective functions, the degree of mixing and pressure drop, were used to define the performance of the micromixer.

It is clear that by optimizing the shape of the grooves, mixing can be effectively increased. As mentioned above, some parametric studies [6–12,20] on the effects of geometric parameters on mixing performance and shape optimization [15–19] have been performed for patterned-groove micromixers. Some studies also have been performed for micromixers with two walls that are patterned by grooves [13,14]. However, systematic techniques of numerical optimization have not yet been applied to micromixers that are patterned by SHGs at both the top and bottom walls. The RSA method [21], which is a global optimization method, has many advantages over gradient-based methods [22] among the methods of numerical optimization that have been used in conjunction with the Navier–Stokes analysis of fluid flows.

In the present work, a numerical optimization model is presented for the shape optimization of a staggered-herringbone micromixer with grooves on both the top and bottom walls. A three-dimensional numerical analysis is performed and the RSA method is employed as an optimization tool to obtain the optimal groove design as well as the optimal number of grooves per cycle. The mixing index is considered as the objective function and four design variables related to micromixer performance, viz., the number of grooves per cycle, angle of grooves, ratio of the groove depth to channel height, and ratio of the groove width to pitch are selected to optimize the mixing performance of the micromixer.

2. Numerical formulation

Fig. 1 shows the schematic diagram of a micromixer with SHG patterns at the top and bottom walls. The main channel is comprised of SHGs and is connected with the two inlet channels with a T-joint. The total length of the channel is fixed at 8.5 mm, which

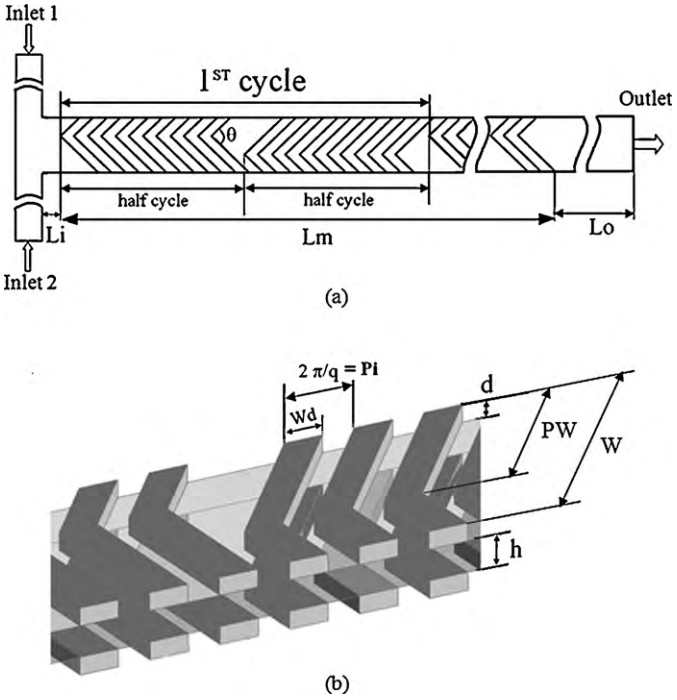

Fig. 1. Geometry of micromixer: (a) schematic of staggered-herringbone groove micromixer and (b) detailed view of SHG structures indicating various design parameters.

is equal to the sum of the various channel-section lengths, i.e., *Li*, *Lm*, and *Lo*, whose dimensions are 0.0632 mm, 5.5 mm, and 2.7 mm, respectively. The width of the inlet channels is 100 μm and the height is equal to that of the main channel. The design of the herringbone grooves is aimed to create strong transverse flow with two large vertices into the microchannel. The off-centre position of the apex of the herringbone grooves defines its asymmetry. Among the geometric variables shown in Fig. 1, the number of grooves per cycle, *N*, ratio of the groove depth to channel height, *d*/*h*, angle of grooves, θ, and ratio of the groove width to pitch, *Wd*/*Pi*, are selected as the design variables for the optimization. The other variables are kept constant: $h = 77\ \mu m$, $W = 200\ \mu m$, $q = 2\pi/100\ \mu m^{-1}$, and $Wd = 50\ \mu m$. The grooves have an asymmetry of *PW*, where *P* is 2/3 [5].

A general purpose CFD code, ANSYS CFX-11.0 [23], has been used to analyze flow and mixing in the micromixers. The solver solves the steady state laminar flow continuity and momentum equations, expressed as:

$$\nabla \cdot \vec{V} = 0 \tag{1}$$

$$\rho(\vec{V} \cdot \nabla)\vec{V} = \nabla p + \mu \nabla^2 \vec{V} \tag{2}$$

The ANSYS CFX-11.0 code solves these equations by using the finite-volume method via a coupled solver. The water and ethanol are selected as two working fluids for mixing. The properties of water and ethanol are taken at 20 °C as shown in Table 1. The uniform velocities at the inlets and zero static pressure at the outlet are specified as the boundary conditions. No slip boundary conditions are assigned at all the channel walls. Pure water is applied at the one inlet while pure ethanol is applied at other inlet. The Reynolds number is calculated based on the dimensions of the channel and properties of water. ANSYS CFX is capable of modeling a fluid mixture that comprises many separate physical components, where each component may have a distinct set of physical properties. To calculate the fluid flow, the CFX solver calculates the average values of the properties for each control volume in the flow domain. These values depend on the values of the componential properties

Table 1
Properties of working fluids at 20 °C.

Fluid	Density (kg m^{-3})	Viscosity (Kg m^{-1} s^{-1})	Diffusivity (m^2 s^{-1})
Water	9.998×10^2	0.9×10^{-3}	1.2×10^{-9}
Ethanol	7.890×10^2	1.2×10^{-3}	1.2×10^{-9}

and the percentage of each component that is present in the control volume. In the case of multi-component fluids, it is assumed that the fluids are mixed at the molecular level and that the properties of the fluids are dependent on the proportions of the components. It is also assumed that the mass-fraction arises through convection and diffusion. The differential motions of individual components in the mixture are computed by relative mass flux terms. The effects of the concentration gradient, pressure gradient, etc., are used to model the relative mass flux.

An unstructured tetrahedral grid system is created for the full model through ANSYS ICEM 11.0 and the quality of the mesh is examined for the accuracy of the numerical model. Navier–Stokes equations in combination with an advection-diffusion model are solved to analyze the actual mixing phenomena. The numerical simulation is not free from numerical diffusion errors, which arise mainly from the discretization of the convection terms in the Navier–Stokes equation. Numerical diffusion cannot be completely ignored; however, it can be minimized by adopting certain techniques [24]. The solutions are considered to have attained convergence when the values of the root-mean-squared (RMS) relative residuals are below 10^{-6}.

The variance of the fluid species in the micromixer has been calculated to quantify and analyze the mixing. The variance of species is determined in a cross-sectional area of the micromixer that is normal to the *x*-axis. The variance is based on the concept of the intensity of segregation, which is based on the variance of the concentration with respect to the mean concentration. To evaluate the degree of mixing in the micromixer, the variance of the mass-fraction of the mixture in a cross-section that is normal to the flow direction is defined as follows.

$$\sigma = \sqrt{\frac{1}{N_o}\sum (c_i - \bar{c}_m)^2} \tag{3}$$

In the above definition, N_o is the number of sampling points inside the cross-section, c_i is the mass-fraction at sampling point *i*, and c_m is the optimal mixing mass-fraction. To quantitatively analyze the mixing performance of the micromixer, the mixing index is defined as follows.

$$M = 1 - \sqrt{\frac{\sigma^2}{\sigma_{max}^2}} \tag{4}$$

In Eq. (4), σ is the standard deviation of the concentration across the channel in a cross-section at any specific longitudinal location, and σ_{max} is the maximum standard deviation (unmixed at the exit). A greater mixing index indicates a higher mixing quality: the value of this mixing index is thus zero for completely separate streams (for which $\sigma = \sigma_{max}$) and unity for completely mixed streams (for which $\sigma = 0$).

3. Optimization methods

The selection of the appropriate design variables that affect the mixing performance is one of the most important aspects of design optimization. In the present study, four design variables as mentioned above are selected to optimize the shape of the micromixer. The design space is selected through some preliminary calculations that are carried out in the light of experimental studies and numerical constraints. Table 2 shows these design variables with their

Table 2
Design variables and their ranges.

	N	θ	d/h	Wd/Pi
Lower bound	5	30	0.2	0.4
Upper bound	15	60	0.6	0.8

ranges, while the other geometric parameters of the microchannel are kept constant.

The optimization problem is defined as the maximization of an objective function, $F(\mathbf{x})$, over $x_i^l \le x_i \le x_i^u$ under equality and inequality constraints. Here, $\mathbf{x}$ is a vector of design variables and x_i^l and x_i^u are the lower and upper bounds of design variable x_i, respectively. To design any micromixer, one of the most important issues is to increase the mixing efficiency of the fluids. Therefore, in this study, the mixing index at the end of the grooves has been employed as the objective function to optimize the shape of the micromixer with SHG patterns at the top and bottom walls.

Generally, optimization algorithms require many evaluations of the objective function to search for optimum solutions in the design space. Therefore, to calculate these objective function values which are required by the search algorithm, a surrogate model is constructed based upon discrete numerical analysis at the selected sites in the design space to avoid experimental or numerical expense and save on computational time. The design of experiments (DOE) is carried out and a Latin hypercube sampling (LHS) design is used to fill up the design space with discrete design sites. The objective functions are calculated by three-dimensional Navier–Stokes analysis at the design points (or experimental points), which are selected through the DOE framework. Then, the surrogate model is constructed based on these objective function values.

The RSA method [21] is an optimization method that is comprised of a series of mathematical and statistical processes. It includes the construction of the response surface by interpolation of the data and optimization of the objective function on the response surface. Polynomial-based response surfaces are commonly employed in the RSM. The polynomial response function used in the present study is defined as follows:

$$\hat{F} = \beta_0 + \sum_{j=1}^{n} \beta_j x_j + \sum_{j=1}^{n} \beta_{jj} x_j^2 + \sum \sum_{i \neq j}^{n} \beta_{ij} x_i x_j \quad (5)$$

where n is the number of design variables and x_i ($i = 1,\ldots, n$) and β_i (or β_{ij}) ($i, j = 1,\ldots, n$) indicate the design variables and regression coefficients, respectively. The number of regression coefficients is $(n+1)\cdot(n+2)/2$. The unknown coefficients of the polynomial are obtained from a standard least-squares regression method by using the calculated responses at the design points. Sequential quadratic programming (SQP) is used as a search algorithm to obtain the optimal shape of the herringbone groove. The search algorithm is triggered for many initial guesses at various locations in the design space to ensure that the optimal design is global in the discrete sense within the design space.

4. Results and discussion

A grid-independency test has been carried out to find the optimal number of grids and ensure that the solution is independent of the grid size. Four different structured grid systems with the number of nodes ranging from 8.43×10^5 to 1.64×10^6 were tested, as shown in Fig. 2. The distribution of the variance of the mass-fraction along the channel was evaluated for various numbers of nodes. Finally, from the results of the grid-independency test, the grid with the number of nodes, 1.32×10^6, was selected as the optimum grid for carrying out further calculations. The validation of the numerical scheme was performed and reported in a previous study [17]. The present numerical scheme used the model of Ansari and Kim [17], which was used for the optimization of a micromixer with SHG patterns at the bottom of the channel.

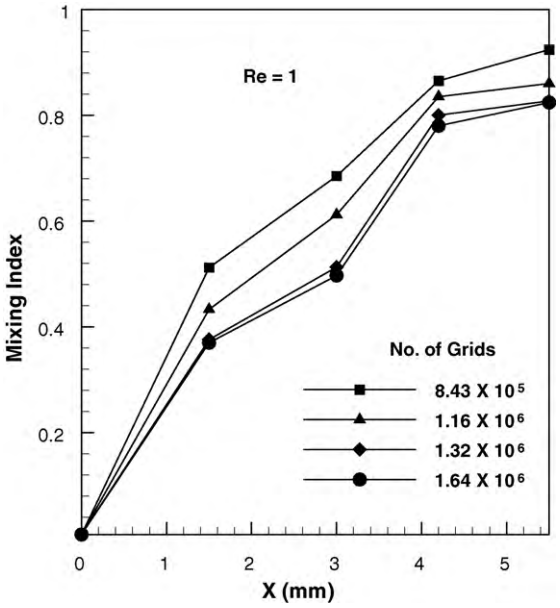

Fig. 2. Grid-independency test at Re = 1.

Fig. 3 presents a comparison of the mixing index across micromixers of smooth microchannel walls, SHGs at the bottom wall, and SHGs at both the bottom and top walls. For the numerical analyses, the Reynolds number, Re, was kept constant at unity. In this comparison, all geometric parameters were kept constant as per the reference design [5]. A very low mixing rate is observed in a microchannel without grooves compared to microchannels with grooves. This difference is attributed to the creation across the direction of flow of two large vortices that are induced by the herringbone grooves on the wall(s), which promote mixing of the two fluids in the cross-flow direction. This figure illustrates that mixing is significantly higher in a micromixer with SHGs at both

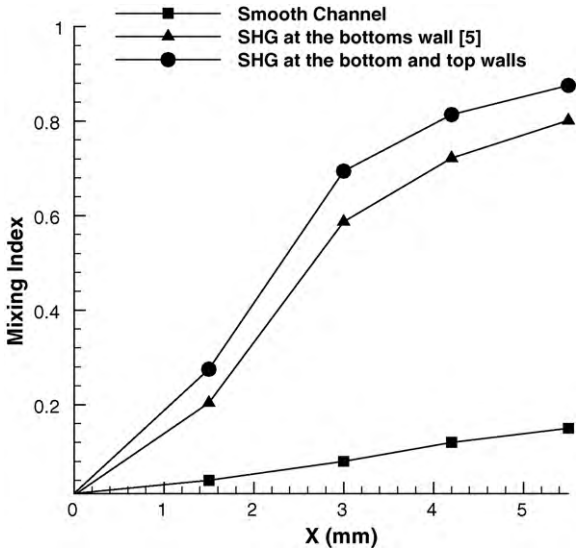

Fig. 3. Mixing index distributions for various micromixers with and without grooves.

Table 3
Comparison of the optimum geometry with the reference geometry (Stroock et. al [5]).

Design variables	N	θ	d/h	Wd/Pi	Objective function	
					Prediction by RSA	Calculation by N–S analysis
Reference geometry	10	45	0.23	0.5	–	0.852
Optimized geometry	15	38.6	0.461	0.56	0.931	0.927

the top and bottom walls than in a micromixer with SHGs at only the bottom wall.

In this work, shape optimization is performed for a micromixer with patterned herringbone grooves at both the top and bottom walls, which is shown in Fig. 1. Two fluids, namely, water and ethanol, are taken as the working fluids. The mixing index at the end of the grooves is used as the objective function, which is to be maximized with respect to four design variables, viz., the number of grooves per half cycle (N), angle of grooves (θ), ratio of the groove depth to channel height (d/h), and ratio of the groove width to groove pitch (Wd/Pi). Response surface-based optimization techniques are used and forty design points are selected by Latin hypercube sampling to construct the response surface for the optimization. From the results of ANOVA and regression analyses [21] for the response surface, the value of R^2_{adj} was determined as 0.932. For accurate prediction of the response surface model, Giunta [25] has suggested that the value of R^2_{adj} should be in the range of $0.9 < R^2_{adj} < 1.0$, which is the case in the present study.

The optimal design is obtained through the constructed surrogate model and SQP. The results of the optimal design are presented in Table 3 along with the reference geometry [5]. The optimal values of the objective function, i.e., the mixing index achieved at the exit, predicted by RSA and calculated by Navier–Stokes analysis are 0.931 and 0.927, respectively. This indicates that RSA shows a 0.5% error in predicting the objective function value at the optimal design. The values of the mixing index achieved at the exit are 0.927 and 0.852 for the optimal and reference designs, respectively. The following formula obtained by RSA is the exemplary functional form of the mixing index as a function of the four design variables in the present design space.

$$y = 0.6319 + 0.0771N + 0.1274\theta + 0.5294\left(\frac{d}{h}\right) + 0.0726\left(\frac{Wd}{Pi}\right) - 0.0759N\theta - 0.0832N\left(\frac{d}{h}\right) - 0.02N\left(\frac{Wd}{Pi}\right) - 0.03\theta\left(\frac{d}{h}\right) - 0.0005\theta\left(\frac{Wd}{Pi}\right) + 0.0081\left(\frac{d}{h}\right)\left(\frac{Wd}{Pi}\right) + 0.0621N^2 - 0.0571\theta^2 - 0.3375\left(\frac{d}{h}\right)^2 - 0.0692\left(\frac{Wd}{Pi}\right)^2 \quad (6)$$

A sensitivity analysis of the objective function is performed by varying the design variables around the optimal design values. Each design variable is varied one at a time from the optimal point in both directions, while the other variables are kept fixed at their respective optimal values. The objective function values at these sets of design variables have been calculated though the surrogate model, RSA (and not through Navier–stokes analysis). Each design variable varies within ±10% of its optimal value. Fig. 4 illustrates that the objective function decreases sharply with the change in d/h when the others design variables are constant. On the other hand, the change in the angle has the smallest effect on the objective function. The optimal N is found at the upper boundary of the selected design space, and therefore, an increase in the value of N monotonically leads to an increase in the mixing index. It should be noted that the surrogate model extrapolates the objective function for the increased value of N beyond the design space, which is not always correct. The sensitivity analysis reveals that the groove angle has the smallest effect on the objective function in the specified range, but the effect of Wd/Pi also is comparable to that of the groove angle.

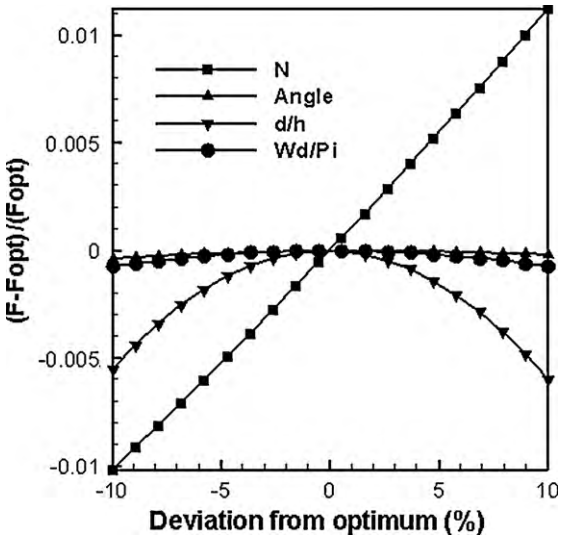

Fig. 4. Sensitvity analysis of the objective function.

Fig. 5 shows the results of a comparative analysis that was performed across the three designs, viz., SHGs at the bottom wall [5], SHGs at both the top and bottom walls, which is a simple modification of the reference geometry [5], and optimized SHGs at both the top and bottom walls. From the figure, it is clear that the optimized geometry shows an almost identical mixing pattern to the reference geometry throughout the channel length. It is clear that the mixing

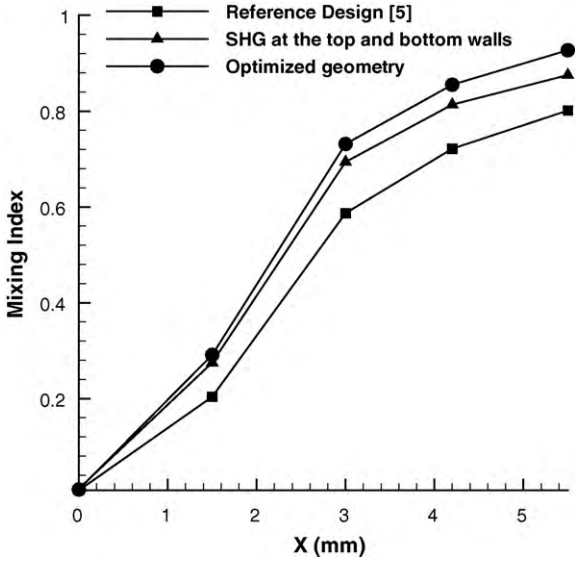

Fig. 5. Mixing index distribution for the reference and optimized micromixers.

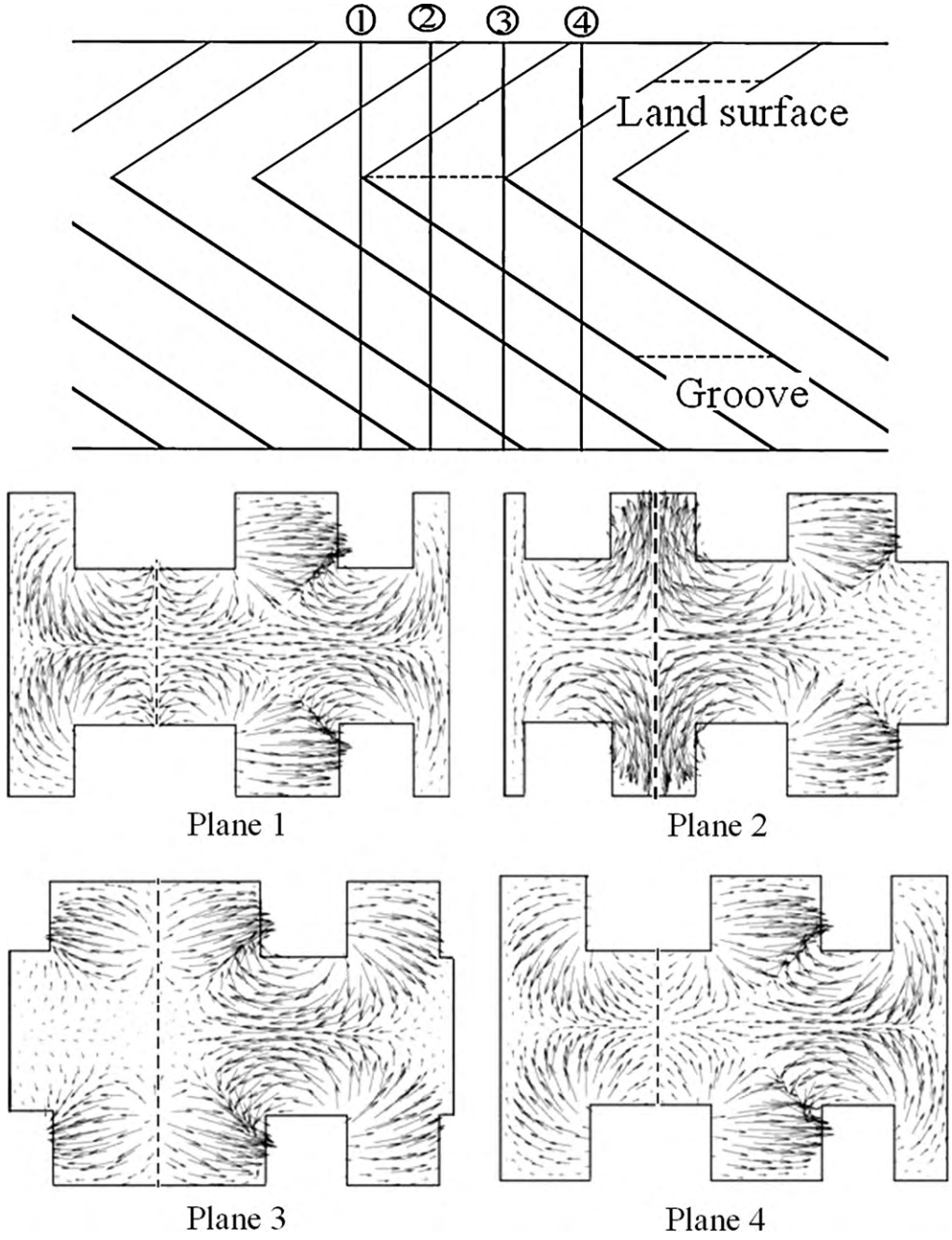

Fig. 6. Velocity vector plots for optimized design of SHG micromixer at various positions.

index is considerably improved throughout the channel length by the optimization. The values of the mixing index achieved at the exit for the optimal and reference geometries represent a relative increase of about 8.8% in the mixing index. In SHG micromixers, transverse flow is created by the angle of grooves, which rotates the stream of fluids throughout the channel length and thereby causes the fluids to mix. For creating maximum transverse flow, Stroock et al. [5] suggested that the angle of grooves be 45°. However, through the optimization, the present study confirms that the optimum groove angle for maximum mixing is 38.6° for grooves that are patterned at both the top and bottom walls.

Fig. 6 shows the velocity vectors on *yz*-planes that are normal to the *x*-direction at various locations in the streamwise direction for the optimized design. These planes are respectively located near the edge of a groove (just before the start of the groove), at the middle of the groove, at the end of the groove, and at the intervening, flat surface between adjacent grooves as indicated by Planes 1–4, respectively. Planes 1, 2, and 4 cut the groove pattern at three different locations, while Plane 3 cuts the groove at two locations. The transverse flow in Plane 1 indicates that the fluid coming out of the right groove reaches to the middle of the channel and the fluids coming out of the left groove and partly from the middle groove mix up in the channel and enter into the next downstream groove. Upon entering into the downstream groove, these two fluid streams mix up in the groove (as shown in Plane 2) and then divide into two parts, while reaching the edge of the groove, as shown in Plane 3. At Plane 3, the figure shows weak secondary flows at the end walls. The fluid that is deflected by the groove reaches to the two extreme walls of the channel and creates chaos in the channel. The fluid that is deflected from the extreme walls enters the groove and

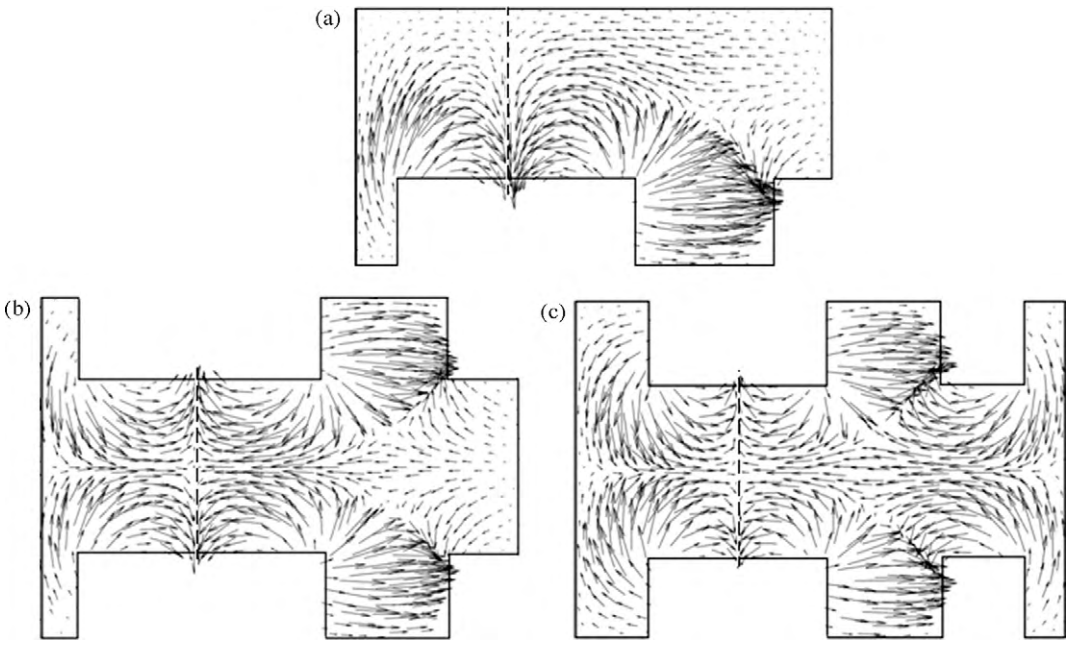

Fig. 7. Comperison of velocity vector plot on yz-plane: (a) reference SHG, (b) reference SHG on both walls, and (c) optimized SHG on both walls.

forms two counter rotating vortices in the channel, which stretches up to the groove edge.

Fig. 7(a–c) presents a comparison of the velocity vector plots across the three designs, namely, SHGs at the bottom wall, SHGs at both the bottom and top walls, and the optimized design of SHGs at both the bottom and top walls, respectively. The velocity vector plane has been selected near the edge of the groove, as seen in Plane 1 in Fig. 6. Fig. 7 shows secondary, induced vortices over the cross-sectional planes. Fig. 7(a) shows secondary, induced vortices near the bottom wall; the flow near the top wall is not affected by the grooves and the vectors are nearly parallel to the wall. Fig. 7(c) represents three grooves and two flat surfaces throughout the cross-sectional plane, while (b) represents two grooves and two flat surfaces. Fig. 7(b) shows weak velocity vectors near the right wall that are due to the flat surface, while under the optimized design of SHGs, strong velocity vectors are deflected towards the middle of the channel. Due to the larger width and depth of the grooves (as shown in Table 3), Fig. 7(c) shows a larger area for mass flow throughout the cross-section of the grooves, which potentially causes a difference in mixing. The optimized geometry capitalizes upon the region near the left wall where the fluid moves towards the middle of the channel with small velocities. The presence of the grooved section near the left wall and the deflection by the wall of fluid that is coming out of the groove create another vortex near the left wall, which enhances the chaos in the channel, as shown in Fig. 7(c). Fig. 7(c) shows that the magnitude of the velocity vector

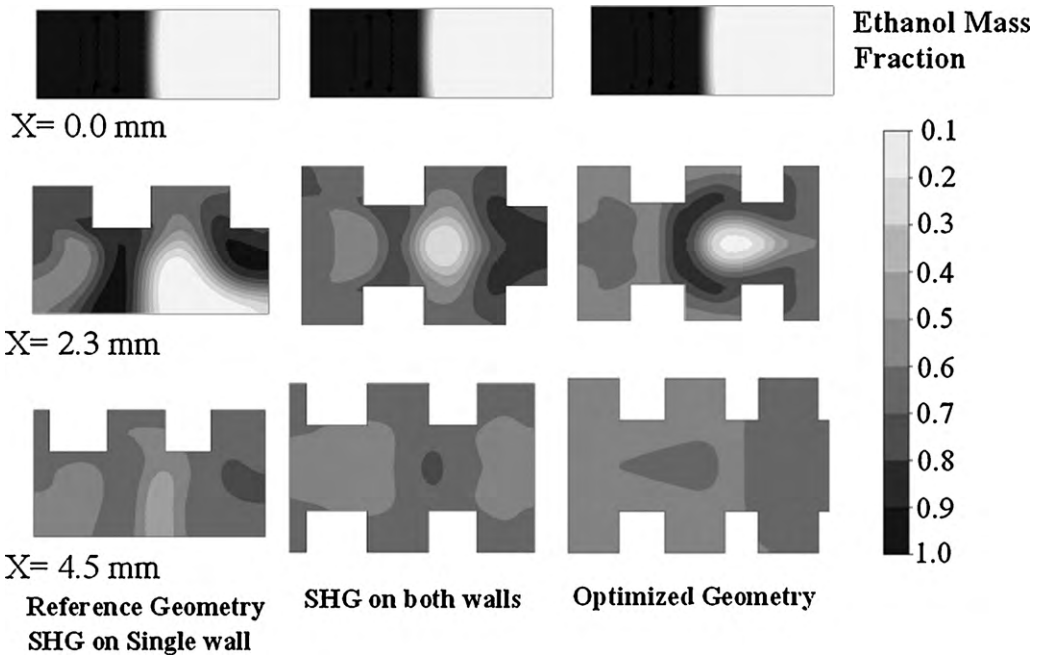

Fig. 8. Mass-fraction distributions of ethanol on cross-stream planes at various streamwise locations in the micromixer for the reference and optimized micromixers.

is relatively uniform throughout the cross-sectional plane, which causes strong secondary flows at the plane in the optimized SHG micromixer.

Fig. 8 presents a comparison of the mass-fraction distributions of ethanol on the planes at various distances along the length of the micromixer for the selected designs. This figure demonstrates a completely unmixed interface at the $x = 0.0$ mm plane in all designs. With an increase in the channel length, the mixing index is increased, as shown in Fig. 5, and the interface of fluids becomes wider. The optimized geometry confirms the most efficient mixing of the two fluids at the exit: more than 90% of mixing is seen at $x = 4.5$ mm in Fig. 5. As the d/h ratio increases, the mass-fraction distributions become more uniform, as reported by Ansari and Kim [17]. The analysis of mass-fraction distributions is also limited by the contrast in the gray-scale in the figures; the contrast is affected by the graphical resolution of the computer hardware.

5. Conclusion

The shape optimization of a micromixer with staggered-herringbone grooves (SHGs) at both the bottom and top walls has been performed using three-dimensional Navier–Stokes analysis and a surrogate model for maximizing the mixing performance. The mixing index at the exit of the micromixer has been taken as the objective function with four design variables, viz., the number of grooves per half cycle, angle of grooves, ratio of the groove depth to channel height, and ratio of the groove width to pitch. The numerical analysis has been performed with two working fluids, viz., water and ethanol, at a Reynolds number of unity. Response surface approximation and sequential quadratic programming are employed as numerical optimization tools to obtain the optimal groove shape as well as the optimal number of grooves per cycle. The micromixer with SHGs patterned at both the bottom and top walls shows higher mixing performance when compared to the reference micromixer with SHGs at a single wall. Furthermore, the optimized micromixer with SHGs at both the bottom and top walls shows an improvement in the mixing performance of about 9% relative to the reference design with grooves at only the bottom wall. Stroock et al. [5] suggested that the angle of grooves be 45° for maximum mixing. However, the present optimization has found that the optimum groove angle for maximum mixing is 38.6° for grooves that are patterned at both the top and bottom walls. Also, the optimal design variable, N, is found at the upper boundary of the design range, which indicates that the mixing can be further enhanced by increasing N –, however this is left unexplored in the present work. A sensitivity analysis reveals that the mixing is much more sensitive to the depth of the groove than either the width or the angle of grooves near the optimal design.

Acknowledgement

This research was supported by the National Research Foundation of Korea (NRF) grant No. 20090083510 funded by government (MEST) through Multi-phenomena CFD Engineering Research Center

References

[1] N.T. Nguyen, Wu, Micromixers – review, J. Micromech. Microeng. 15 (2005) 1–16.
[2] D. Erickson, Towards numerical prototyping of labs-on-chip: modeling for integrated microfluidic devices, Microfluidics Nanofluidics 1 (2005) 301–318.
[3] V. Vivek, Y. Zeng, E.S. Kim, Novel acoustic-wave micromixer, in: Proceedings of the IEEE Micro Electro Mechanics System (MEMS), 2000, pp. 668–673.
[4] J. Cao, P. Cheng, F.J. Hong, A numerical study of an electrothermal vortex enhanced micromixer, Microfluidics Nanofluidics 5 (2008) 13–21.
[5] A.D. Stroock, S.K. Dertinger, A. Ajdari, I. Mezic, H.A. Stone, G.M. Whitesides, Chaotic mixer for microchannels, Science 295 (2002) 647–651.
[6] H. Wang, P. Ioveitti, E. Harvey, S. Masood, Numerical investigation of mixing in microchannels with patterned grooves, J. Micromech. Microeng. 13 (2003) 1397–1405.
[7] Y.Z. Liu, B.J. Kim, H.J. Sung, Two fluid mixing in microchannel, Int. J. Heat Fluid Flow 25 (2004) 986–995.
[8] T.G. Kang, T.H. Kwon, Colored particle tracking method for mixing analysis of the chaotic micromixers, J. Micromech. Microeng. 14 (2004) 891–899.
[9] J.T. Yang, K.J. Huang, Y.C. Lin, Geometric effects on fluid mixing in passive grooved micromixers, Lab Chip (2005), doi:10.1039/b500972c.
[10] J. Aubin, D.F. Fletcher, C. Xuereb, Design of micromixer using CFD modeling, Chem. Eng. Sci. 60 (2005) 2503–2516.
[11] Y. Tang, J. Wu, E. Czyzewska, K. Stanley, An optimized micromixer with patterned grooves, in: Proceedings International Conference on MEMS, NANO and smart systems (ICMENS'04), 2010.
[12] D.G. Hassell, W.B. Zimmerman, Investigation of the convective motion through a staggered herringbone micromixer at low Reynolds number flow, Chem. Eng. Sci. 61 (2006) 2977–2985.
[13] P.B. Howell Jr., M.R. David, S. Fertig, C.R. Kaplan, J.P. Golden, E.S. Oran, F.S. Ligler, A microfluidic mixer with grooves placed on the top and bottom of the channel, Lab Chip 5 (2005) 524–530.
[14] J.T. Yang, W.F. Fang, K.Y. Tung, Fluids mixing in devices with connected-groove channels, Chem. Eng. Sci. 63 (2008) 1871–1881.
[15] T.J. Johnson, L.E. Locascio, Characterization and optimization of slanted well designs for microfluidic mixing under electroosmotic flow, Lab Chip 2 (2002) 135–140.
[16] M.A. Ansari, K.Y. Kim, Application of the radial basis neural network to optimization of a micromixer, Chem. Eng. Technol. 30 (7) (2007) 962–966.
[17] M.A. Ansari, K.Y. Kim, Shape optimization of a micromixer with staggered herringbone groove, Chem. Eng. Sci. 62 (2007) 6687–6695.
[18] N.S. Lynn, D.S. Dandy, Geometrical optimization of helical flow in grooved micromixers, Lab Chip (2007), doi:10.1039/b700811b.
[19] H. Song, X.Z. Yin, D.J. Bennett, Optimization analysis of the staggered herringbone micromixer based on the slip-driven method, Chem. Eng. Res. Des. 86 (2008) 883–891.
[20] C.A.C. Quiroz, M. Zangeneh, A. Goto, On multi-objective optimization of geometry of staggered herringbone micromixer, Microfluidics Nanofluidics (2009), doi:10.1007/s10404-008-0355-8.
[21] R.H. Myers, D.C. Montgomery, Response Surface Methodology: Process and Product Optimization using Designed Experiment, Wiley, New York, 1995.
[22] G.N. Vanderplaats, Numerical Optimization Techniques for Engineering Design with Applications, McGraw-Hill, New York, 1984.
[23] CFX-11.0, Solver Theory, ANSYS, 2007.
[24] S. Hardt, F. Schonfeld, Laminar mixing in different interdigital micromixers. II. Numerical Simulations, AICHE J. 49 (3) (2003) 578–584.
[25] A.A. Giunta, Aircraft Multidisciplinary Design Optimization using Design of Experiments Theory and Response Surface Modeling Methods, Ph.D. Thesis, Department of Aerospace Engineering, Virginia Polytechnic Institute and State University, Blacksburg, Virginia, 1997.